

See discussions, stats, and author profiles for this publication at: <https://www.researchgate.net/publication/231647293>

The Effect of the Reduction of the Available Surface Area on the Hemicyanine Aggregation in Laterally Organized Langmuir Monolayers

ARTICLE *in* THE JOURNAL OF PHYSICAL CHEMISTRY C · APRIL 2011

Impact Factor: 4.77 · DOI: 10.1021/jp200769g

CITATIONS

8

READS

29

7 AUTHORS, INCLUDING:



Juan Giner-Casares

CIC biomaGUNE

46 PUBLICATIONS 283 CITATIONS

SEE PROFILE



Pérez-Morales Marta

University of Cordoba (Spain)

30 PUBLICATIONS 270 CITATIONS

SEE PROFILE



Luis Camacho

University of Cordoba (Spain)

150 PUBLICATIONS 1,570 CITATIONS

SEE PROFILE

The Effect of the Reduction of the Available Surface Area on the Hemicyanine Aggregation in Laterally Organized Langmuir Monolayers

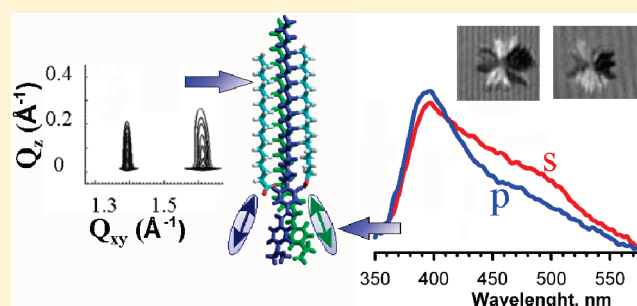
Antonio M. González-Delgado,[†] Juan J. Giner-Casares,^{†,‡} Carlos Rubia-Payá,[†] Marta Pérez-Morales,[†] María T. Martín-Romero,[†] Gerald Brezesinski,[‡] and Luis Camacho^{*,†}

[†]Department of Physical Chemistry and Applied Thermodynamics, Andalusian Institute of Fine Chemistry and Nanochemistry (IAQFN), University of Córdoba, Campus de Rabanales, Edificio Marie Curie, Córdoba, Spain E-14014

[‡]Interfaces Department, Max Planck Institute of Colloids and Interfaces, Science Park Golm, 14476 Potsdam, Germany

S Supporting Information

ABSTRACT: This paper analyzes the effect of the reduction of the available area on the aggregation of an hemicyanine dye, 4-[4-dimethylamino]styryl]-1-docosylpyridinium bromide (SP), at the air–water interface. Mixed films of SP and stearic acid (SA) in 1:1 molar ratio have been studied, and compared with the previously studied films of SP and dimyristoyl-phosphatidic acid (DMPA) in 1:1 molar ratio. With regard to the SP:DMPA films, the replacement of DMPA by SA involves reducing the area available for the hemicyanine aggregation, since the SA molecule provides only an alkyl chain to the set, whereas the DMPA molecule provides two alkyl chains to the set. The SP:SA mixed films have been studied by Grazing Incidence X-ray Diffraction (GIXD), Brewster angle microscopy (BAM), and reflection spectroscopy at the air–water interface. Langmuir–Schaeffer films have been studied by UV–vis transmission spectroscopy. The SP:SA mixed monolayer forms star-shaped domains with inner textures, indicating anisotropy. Circular domains were observed for the SP:DMPA system. GIXD experiments relate the star-shaped domains with an orthorhombic phase, as for circular domains observed for the SP:DMPA system. The results obtained by reflection and transmission polarized spectroscopy for the SP:SA system showed the splitting of the absorption band of the aggregate. The splitting has been related with a twisting in the hemicyanine groups. The reduction on the available area accounts for the aggregation of the hemicyanine group. The domain shape at the mesoscopic level mainly originated from the interactions between the polar groups and the reduced surface area. The interactions between the alkyl chains are essential to maintain the crystalline structure, although these interactions did not play the main role in the final shape of the domain.



INTRODUCTION

In Langmuir monolayers, the repulsive dipolar interaction of the molecules within a domain favors a large boundary-to-area ratio, by which the electrostatic repulsion energy is reduced.¹ In this case, the domain morphology does not entirely correspond to the molecular lattice structure. To design well-defined structures, in which the lateral organization is controlled, it is required to compensate the repulsion energy between dipoles. To achieve this compensation, the polar heads of lipids should be connected, either through hydrogen bonding,² or through the self-aggregation of dyes.^{3,4} Recently, we have used the latter strategy to study mixed films containing dimyristoyl-phosphatidic acid (DMPA) and an amphiphilic hemicyanine dye (SP) in a 1:1 molar ratio.⁴

The key to apply this procedure is the adequate balance between the sizes of the hydrophobic and hydrophilic groups. The DMPA plays a triplet role in the SP:DMPA = 1:1 films. First, the DMPA molecule provides two aliphatic chains to the set, so the minimum

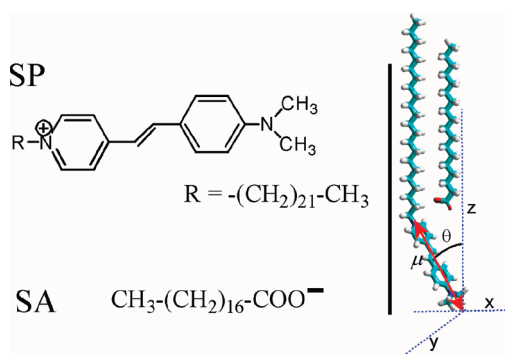
perpendicular section of the 1:1 mixture would be around 0.6 nm² per SP molecule. Second, the anionic DMPA offsets the positive charge of the SP molecule. Finally, the alkyl chains of the DMPA are shorter than those of the SP, so that the DMPA polar group does not avoid the hemicyanine aggregation by the dye molecular tilt. Thus, if a_c is the interfacial area occupied by the hydrophobic group when the alkyl chains are fully extended ($a_c \approx 0.6$ nm² in the SP:DMPA = 1:1 system), and a_0 is the minimum interfacial area occupied by the headgroup ($a_0 \approx 0.33$ nm² for the hemicyanine group), the dyes to be selected should obey $a_c \geq a_0$. In this way, the domain structure depends on the ability of the dye to fill the available area excess ($a_c - a_0$).⁴ BAM images show a well-organized structure (circular domains) of micrometre size, which presents

Received: December 11, 2010

Revised: April 8, 2011

Published: April 21, 2011

Scheme 1. Molecular Structures of Hemicyanine, SP, and Stearic Acid, SA^a



^a Graphical definition of the transition dipolar moment, μ , the polar tilt angle, θ , of the SP molecules in the presence of the SA molecule (the interface plane coincides with the x - y plane) are given.

inner anisotropy. By Grazing Incidence X-ray Diffraction (GIXD), the formation of two different crystalline phases, orthorhombic and Overbeck, was observed. The orthorhombic phase showed no tilting of hydrocarbon chains, whereas in the Overbeck phase the tilting value was ca. 17° for the complete range of surface pressure studied. Moreover, information on the organization of the polar heads was obtained by using reflection spectroscopy and simulating the domains observed.

In this paper, mixed films containing SP and stearic acid (SA) in a 1:1 molar ratio (see Scheme 1) have been studied. With regard to the previous study of the SP: DMPA = 1:1 films, the replacement of DMPA by SA involves the reduction of the available area for the hemicyanine aggregation, since each SA provides only an alkyl chain to the set. Therefore, the minimum perpendicular section of the 1:1 mixture would be ca. 0.4 nm^2 per SP molecule. The SA molecule, as in the case of the DMPA molecule, can offset the positive charge of SP, as it is negatively charged at neutral pH. The alkyl chain of SA is also shorter than that of SP. These features do not avoid the hemicyanine aggregation by the dye molecular tilt.

The present study attempts to analyze the effect of the reduction of the available space in both the structure of domains formed and the hemicyanine aggregation. Information on the possible changes in the packing of the alkyl chains is also analyzed. Thus, the molecular organization and the domain morphology of SP:SA = 1:1 mixed films have been studied by using Grazing Incidence X-ray Diffraction (GIXD), Brewster angle microscopy (BAM), and reflection spectroscopy at the air–water interface, as well as transmission spectroscopy of the monolayers transferred onto quartz.

The BAM images of the SP:SA = 1:1 system show the formation of star-shaped domains, with different geometry when compared to those observed for the SP:DMPA system. Moreover, the GIXD experiment permitted us to relate the star-shaped domains with an untilted conformation of the hydrocarbon chains, which adopt a solid condensed state along the whole isotherm. Also, the closer approach between the hemicyanine groups led to a surprising phenomenon barely perceptible in the SP:DMPA system: the splitting of the absorption band of the aggregate. This splitting of the band has been related to a molecular distribution in which the hemicyanine groups are not organized parallel, but slightly twisted to each other. Therefore, the corresponding transition dipoles are added, resulting in

two components or excited states with perpendicular orientation and optically allowed.^{5–7}

EXPERIMENTAL SECTION

Materials. Hemicyanine dye, 4-[4-(dimethylamino)styryl]-1-dodecylpyridinium bromide (SP), and stearic acid (SA) were purchased from Sigma-Aldrich and used as received. Their molecular structures are depicted in Scheme 1. A mixture of chloroform:methanol, ratio 3:1 (v/v), was used as spreading solvent for solving both components. The pure solvents were obtained without purification from Aldrich (Germany). Ultrapure water, produced by a Millipore Milli-Q unit, pretreated by a Millipore reverse osmosis system ($>18.2 \text{ M}\Omega \text{ cm}$), was used as a subphase. The subphase pH was 5.7 and the temperature was externally controlled.

Methods. Two different models of Nima troughs (Nima Technology, Coventry, England) were used in this work, both provided with a Wilhelmy type dynamometric system using a strip of filter paper: a NIMA 611D with one moving barrier for the measurement of the reflection spectra, and a NIMA 601, equipped with two symmetrical barriers to record BAM images. The monolayers were compressed at a speed of $\sim 0.1 \text{ nm}^2 \text{ min}^{-1} \text{ molecule}^{-1}$.

UV–visible reflection spectra at normal incidence as the difference in reflectivity (ΔR) of the dye film-covered water surface and the bare surface⁸ were obtained with a Nanofilm Surface Analysis Spectrometer (ref SPEC,² supplied by Accurion GmbH, Göttingen, Germany). The reflection spectra were normalized to the same surface density of hemicyanine by multiplying ΔR by the surface area, i.e., $\Delta R_{\text{norm}} = \Delta R \cdot A$, where A ($\text{nm}^2/\text{SP molecule}$) is taken from the surface pressure–area (π - A) isotherms. UV–visible electronic absorption spectra of the films were measured locating the substrate directly in the light path on a Cary 100 Bio UV–visible spectrophotometer.

Images of the film morphology were obtained by Brewster angle microscopy (BAM) with a I-Elli2000 (Accurion GmbH) using a Nd:YAG diode laser with wavelength 532 nm and 50 mW, which can be recorded with a lateral resolution of $2 \mu\text{m}$. The image processing procedure included a geometrical correction of the image, as well as a filtering operation to reduce interference fringes and noise. The microscope and the film balance were located on a table with vibration isolation (antivibration system MOD-2 S, Accurion, Göttingen, Germany) in a large class 100 clean room.

The monolayers were transferred onto quartz substrates, cleaned in successive steps with an alkaline detergent, isopropanol, and ethanol, and then rinsed with ultrapure water. The monolayers were transferred at constant surface pressure by the Langmuir–Schaeffer technique, i.e., by horizontal touching of the substrate and the interface covered with the mixed film. The multilayers were assembled by sequential monolayer transfer. The transfer ratio was close to unity for all transfer processes.

Grazing Incidence X-ray Diffraction (GIXD) measurements of the monolayer were performed at 21°C at the BW1 beamline, HASYLAB, DESY (Hamburg, Germany). A Langmuir film balance equipped with a single movable barrier and a Wilhelmy plate for monitoring the lateral pressure was placed in a hermetically closed container filled with helium. At BW1, a monochromatic synchrotron X-ray beam ($\lambda = 1.304 \text{ \AA}$) was adjusted to strike the helium/water interface at a grazing incidence angle $\alpha_i = 0.85\alpha_c$ ($\alpha_c = 0.13^\circ$) and illuminated roughly $2 \times 50 \text{ mm}^2$ of the surface. During the measurements, the trough was laterally moved to avoid any sample damage by the strong X-ray beam. A linear position-sensitive

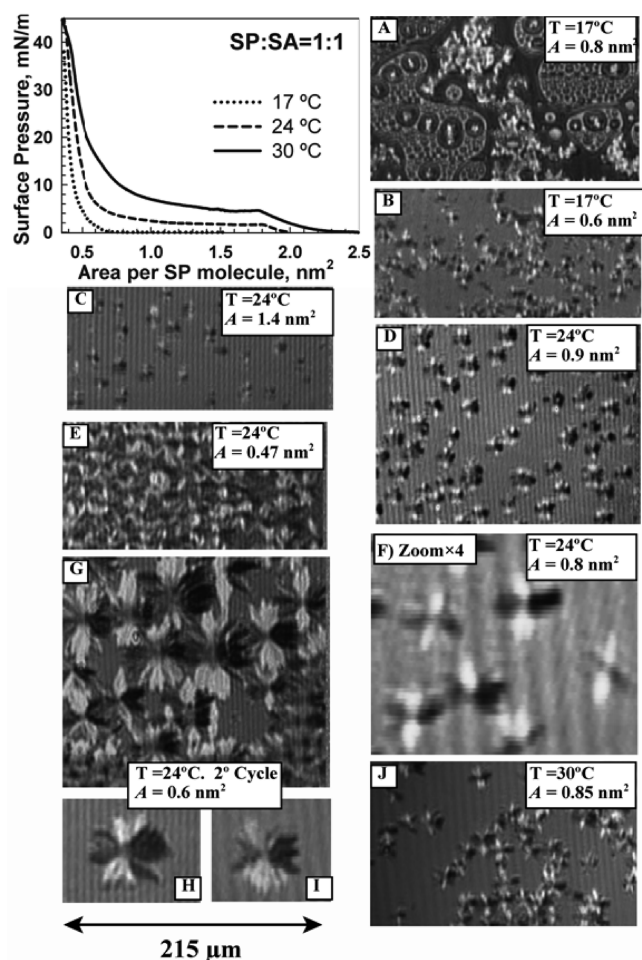


Figure 1. Surface pressure–area (π – A) isotherms of the mixed SP:SA monolayer in a 1:1 molar ratio at $T = 17$, 24, and 30 °C (top left). (A–J) BAM images of the mixed SP:SA = 1:1 monolayer under different surface pressures and temperatures at the air–water interface. Image size: 215 μm width.

detector (PSD, MYTHEN, Switzerland) was rotated to scan the in-plane Q_{xy} component values of the scattering vector. The vertical channels of the PSD measured the out-of-plane Q_z component of the scattering vector between 0 and 0.8 \AA^{-1} . The diffraction data consisted of Bragg peaks at diagnostic Q_{xy} values. The accumulated position-resolved counts were corrected for polarization, effective area, and Lorentz factor. Model peaks taken as Lorentzian in the in-plane direction and as Gaussian in the out-of-plane direction were least-squares fitted to the measured intensities. The diffracted intensity normal to the interface was integrated over the Q_{xy} window of the diffraction peak to calculate the corresponding Bragg rod. Experimental details are described in the literature.^{9–14}

Infrared Reflection Absorption Spectroscopy (IRRAS) spectra were recorded on an IFS 66 FT-IR spectrometer (Bruker, Germany) equipped with a liquid nitrogen-cooled MCT (mercury cadmium telluride) detector. The spectrometer was coupled to a Langmuir–film balance, placed in a sealed container, to guarantee a constant-vapor atmosphere (the external XA-511 air/water reflection unit). In a typical experiment, 1 h was given to saturation of the atmosphere with water vapor. Within the container, a wet paper filter was placed to ensure the saturation of water vapor. The IR beam was conducted out of the spectrometer

and focused onto the water surface of the Langmuir trough. A computer-controlled rotating KRS-5 wire-grid polarizer (thallium bromide and iodide mixed crystal) was used to generate parallel (p) and perpendicular (s) polarized light. The angle of incidence was set to 40° with respect to the surface normal. Measurements were performed with use of a trough with two connected compartments and a trough shuttle system.^{15,16} One compartment contained the monolayer system under investigation (sample), whereas the other (reference) was filled with the pure subphase. The single-beam reflectance spectrum of the reference trough surface was used as the background signal to the single-beam reflectance spectrum of the sample to calculate the reflection absorption spectrum as $(-\log(R/R_0))$. IR spectra were collected at 8 cm^{-1} resolution, using 200 scans for s-polarized light and 400 scans for p-polarized light.

RESULTS AND DISCUSSION

1. Surface Pressure–Area Isotherms and Brewster Angle Microscopy (BAM). Monolayers of SP:SA = 1:1 have been formed at the air–water interface by the cospreading method. Figure 1 (top left) shows the π – A isotherms at 17, 24, and 30 °C for the SP:SA = 1:1 monolayer. For $T \geq 24$ °C and area values close to 1.8 nm^2 , a phase change is observed. All the isotherms converged at high surface pressures reaching at a surface pressure of 35 mN/m, surface areas of 0.37, 0.4, and 0.44 nm^2 , for $T = 17$, 24, and 30 °C, respectively. These surface area values are consistent with the presence of two alkyl chains per hemicyanine group.

Simultaneously to the isotherm recording, the morphology of the mixed monolayer at the air–water interface was directly observed by BAM. At $T = 17$ °C and very low surface pressure (Figure 1A), the monolayer appeared to be composed of a mixture of gas phase and bright domains. The appearance of domains indicates a strong aggregation of the hemicyanine group. When the surface area decreased, the monolayer appears homogeneous, indicating the complete miscibility of the components. After the isotherm takeoff, small domains could be observed (Figure 1B). The morphology of these small domains could not be clearly observed, although they showed different textures with brighter and darker regions than the surrounding background. At high surface pressure, these structures occupied the entire observed region.

At $T = 24$ °C and for areas slightly above the phase change, the monolayer is homogeneous. For areas below the phase change, small domains similar to those described in Figure 1B appeared. When the area was further reduced, the domains grew in size (Figure 1, panels C and D). At high surface pressure, the domains eventually covered the entire observed region (Figure 1E). Figure 1F shows the enlargement (zoom) of a BAM image in the early stages of the domain growth. The domains appeared as 4-pointed stars. The number of points increased as the surface pressure was increased, and these points are not symmetrically distributed in space. The star-shaped domains have inner textures, with different brightness. The vertical points of the star are brighter than the environment, while the lateral points of the star are darker. In a BAM experiment, p-polarized light reaches the air–water interface with an incidence angle of 53.15°, the Brewster angle for the air/water interface. Usually, the different BAM textures are observed due to changes of the refractive index resulting from differences in thickness, density, and/or molecular orientation between the different regions of the film. However, in our case the SP molecules absorb at the wavelength of the laser incident (532 nm, see Figure 4 below). This phenomenon was the main

cause of the high reflectivity observed in the monolayer.^{3,4} As in the SP:DMPA system, hemicyanine aggregation induced the formation of domains. The inner texture is an indication of an ordered aggregation of these groups (anisotropy). In other words, the different textures observed in the domains can be related to the 2D order of the polar groups of the monolayer.⁴

The BAM images shown in panels C–F in Figure 1 correspond to the π –A isotherm at 24 °C, during the first compression cycle. When the monolayer was decompressed and a second compression process was performed, some hysteresis at low surface pressure happened. Both isotherms were coincident at high surface pressure. The hysteresis at low surface pressure was related to the fact that the domains did not disappear completely when the monolayer was expanded. However, a significant phenomenon was observed during the second compression process: the domains growth is larger than in the first cycle (see Figure 1, panels G, H, and I). Note that these domains coexisted with irregular structures (images not

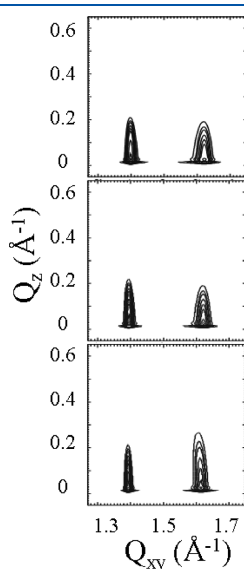


Figure 2. Contour plots of the corrected X-ray intensities as a function of the in-plane and out-of plane scattering vector Q_{xy} and Q_z components for the mixed SA:SP monolayer in a 1:1 molar ratio at $T = 21$ °C. The GIXD measurements were performed at different values of surface pressure. From bottom to top: 3, 10, and 25 mN/m.

Table 1. In-Plane Q_{xy} and Out-of-Plane Q_z Components of the Scattering Vector of the Mixed SA:SP Monolayer in a 1:1 Molar Ratio at $T = 21$ °C^a

π , mN m ⁻¹	Q_{xy} , Å ⁻¹	Q_z , Å ⁻¹	Q_{xy} , Å ⁻¹	Q_{z1} , Å ⁻¹
3	1.393 (0.011)	0 (0.2)	1.612 (0.026)	0.080 (0.23)
10	1.395 (0.012)	0 (0.197)	1.620 (0.026)	0 (0.22)
25	1.398 (0.013)	0 (0.190)	1.620 (0.027)	0 (0.22)

^aThe full-width at half-maximum (fwhm) of the peaks is given in parentheses.

Table 2. Primitive Unit Cell Parameters, Distortion Values, Tilt Angle, Projection of Hydrocarbon Chains in the xy Plane (A_{xy}), and Cross Sectional Area of Hydrocarbon Chains (A_0) of the Mixed SP:SA Monolayer in a 1:1 Molar Ratio at $T = 21$ °C

π , mN m ⁻¹	a , Å	$b = c$, Å	α , deg	$\beta = \gamma$, deg	distortion	tilt angle, deg	A_{xy} , Å ²	A_0 , Å ²
3	4.322	5.001	128.8	115.6	0.1844039	3.1	19.5	19.5
10	4.297	4.990	129.0	115.5	0.1885730	0	19.4	19.4
25	4.299	4.982	128.9	115.6	0.1860272	0	19.3	19.3

shown). In these large domains, the properties previously described appear. The domains showed anisotropy, and the variation of the polarization of the BAM laser changed their texture. At $T = 30$ °C, the features observed in the domains were similar, but slightly larger than those recorded at 24 °C, as shown in Figure 1J.

Additionally, experiments for the SP:SA = 1:1 monolayer with use of a buffered subphase (acetic acid/acetate 10^{-5} M) were carried out. Isotherms and BAM images did not show any difference from those obtained by using pure water as a subphase.

The morphology of the domains observed in the presence of SA was different from those in the presence of DMPA. Thus, circular domains with bright horizontal regions and dark vertical regions have been observed for the SP:DMPA = 1:1 film.⁴ Furthermore, a modification of the temperature leads to a growth of branches from circular domains, whose brightness depended on the growth direction. In the presence of SA, there were star-shaped domains, indicating a different organization, at least with respect to the polar groups.

2. Synchrotron Grazing Incidence X-ray Diffraction (GIXD). Grazing Incidence X-ray Diffraction (GIXD) measurements have been performed in order to obtain quantitative information about the 2D symmetry of Langmuir monolayers. GIXD is sensitive only to the condensed parts of the monolayer, giving an ordered structure that can result in X-ray diffraction. The liquid expanded phase contributes only to the background scattering. Structural changes along compression occurring for the SP/SA mixed monolayer have been monitored.

The crystalline phases of stearic acid have been described along monolayer compression as L_2 –Ov–LS.^{17,18} The transition surface pressure into the nontilted LS phase is 24.6 mN/m. Figure 2 shows the corrected X-ray intensities as a function of the scattering vector components Q_{xy} and Q_z for the mixed SP:SA monolayer in a 1:1 molar ratio at $T = 21$ °C. The X-ray diffraction patterns have been recorded at three different surface pressures: 3, 10, and 25 mN/m. In the investigated interval of surface pressures, there are two clear and well-defined Bragg peaks. Diffraction peaks and rods values are depicted in Table 1, with their full-width at half-maximum (fwhm) values. Quantitative information on the unit cell parameters, tilt angle, and cross sectional area can be found in Table 2. The observed nearest neighbor (NN) tilt direction coupled with a next-nearest neighbor (NNN) unit-cell distortion direction is described as a L_{2h} .¹⁴ Therefore, the mixed monolayer SP:SA adopts a L_{2h} phase at low values of surface pressure. Above the phase transition surface pressure of ca. 5 mN/m, the mixed monolayer SP:SA exhibits a nontilted condensed phase with an orthorhombic unit-cell. Calculating the orthorhombic unit-cell parameters a and b shows that the packing mode is pseudoherringbone. The unit-cell distortion is in the NNN direction. To the best of our knowledge, no untilted phase with NNN distortion has been previously described.¹⁴ Therefore, the known nomenclature cannot be used.

The hydrocarbon chain lengths of SP (C22) and SA (C18) are quite similar. Enough space underneath the SA headgroup is expected to accommodate the bulky headgroup of SP. Therefore,

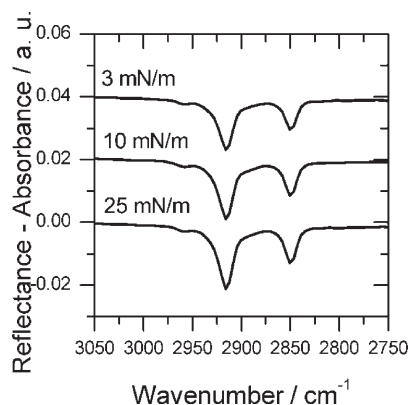


Figure 3. Selected region of IRRA spectra from the mixed SA:SP monolayer in a 1:1 molar ratio at $T = 21\text{ }^{\circ}\text{C}$, at different surface pressures. Spectra have been collected at an incidence angle of 40° by using p-polarized light. For clarity the spectra are scaled with an offset of cumulative 0.02 a.u.

a well-packed, highly crystalline structure of the mixed monolayer is obtained. However, unlike other mixed monolayers composed of two similar surfactants, the headgroups are very different. The arrangement of the bulky SP headgroup might induce the NNN distortion of the lattice.

The tight packing of the monolayer has also been confirmed by IRRAS. Figure 3 shows the IRRAS spectra of the mixed monolayer at 3, 10, and 25 mN/m. For the complete range of surface pressures, similar results on hydrocarbon chains conformation have been obtained. The asymmetric stretching mode of methylene, $\nu_{\text{as}}(\text{CH}_2)$, shows values of 2915.8, 2915.9, and 2915.9 cm^{-1} for 3, 10, and 25 mN/m, respectively. The symmetric stretching mode of methylene, $\nu_{\text{s}}(\text{CH}_2)$, shows values of 2849.7, 2849.8, and 2849.9 cm^{-1} for 3, 10, and 25 mN/m, respectively. Therefore, the low wave numbers in the region of the CH_2 stretching vibrations show that the hydrocarbon chains of both SP and SA are tightly packed in the condensed state along the complete isotherm. The most prominent band in the spectra is that at 3580 cm^{-1} that arises from the OH stretch of water and is a characteristic feature of IRRA spectra (see the Supporting Information). The water OH stretching vibration present in the reference signal (R_0) is reduced in the reflectivity signal from the monolayer-covered surface (R) because the lipid layer replaces a water layer and masks partially the OH stretching vibration. The result is a strong positive band at 3580 cm^{-1} that is related to the monolayer's effective thickness. As expected from the GIXD results showing small or no tilt angles, the intensity of this band does not change remarkably because the layer thickness and the packing density are mostly constant in the investigated pressure range. Surprisingly, the splitting of the CH_2 deformation band, expected from the GIXD results because of the packing in an orthorhombic unit cell, is not observed. Instead, a single band at 1472 cm^{-1} can be seen at all pressures (see the Supporting Information). The band at ca. 1166 cm^{-1} is assigned to the C–O stretch vibration mode of the carboxylic group of stearic acid.¹⁹

3. Reflection Spectroscopy of the Mixed SP:SA Monolayers. The normalized reflection spectra, ΔR_{norm} , of SP:SA = 1:1 monolayers on water subphase at different surface areas (see isotherm of Figure 1) are shown in Figure 4.

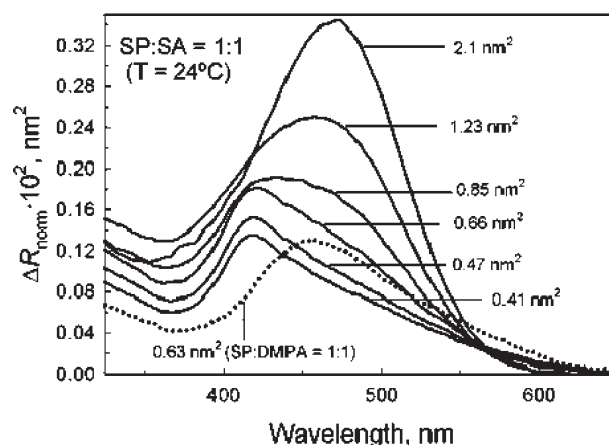


Figure 4. Normalized reflection spectra, ΔR_{norm} , of the mixed SP:SA = 1:1 monolayers (solid lines). The surface areas are indicated in the figure. For comparison, the normalized reflection spectrum of the mixed SP:DMPA = 1:1 monolayer at high surface pressure (0.63 nm^2 per SP molecule) is also shown (dotted line).

For low values of absorption, the reflection ΔR has been shown to be proportional to the surface concentration of the dye.^{8,20–22} In this case, the corresponding product $\Delta R \cdot A = \Delta R_{\text{norm}}$ could be expressed by⁴

$$\Delta R_{\text{norm}} = \Delta R \cdot A = (5.407 \times 10^{-8}) f_{\text{orient}} \epsilon \quad (1)$$

where the extinction coefficient ϵ is given as $\text{L mol}^{-1} \text{ cm}^{-1}$, f_{orient} is a numerical factor that takes into account the different average orientation of the square transition moment of the dye in solution as compared to the monolayer at the air–water interface, A is the surface area per dye molecule, and ΔR_{norm} is expressed in nm^2 .

At low surface pressures, the spectra presented a low-energy band at 475 nm, corresponding to the π – π^* transition of the chromophore in trans configuration.^{23,24} As the surface pressure increased, two phenomena were observed in the reflection band:

(1) The maximum wavelength of the band was shifted to shorter wavelengths, from 475 to 410 nm (in the case of the SP:DMPA system, the band shifted from 475 to 459 nm). This shift is attributed to the formation of H aggregates of the SP chromophores.^{23–26} For comparison, Figure 4 shows the reflection spectrum of the SP:DMPA = 1:1 mixed monolayer, taken at a surface area close to the collapse of the film. In the vicinity of the collapse, the area per hemicyanine group was lower in the SP:SA film ($\sim 0.4\text{ nm}^2$) than in the SP:DMPA film ($\sim 0.6\text{ nm}^2$). Therefore, the hemicyanine groups seemed to be closer in the SP:SA system, which led to a greater interaction between them.

(2) ΔR_{norm} decreased under compression, which could be related to the decreasing of the polar tilt angle of the chromophores. The polar angle θ is defined as the angle between the SP transition moment and the normal to the air–water interface (see Scheme 1). As demonstrated previously for the SP:DMPA system,⁴ the integration of the absorption band gives the apparent oscillator strength. The value of the polar angle θ can be calculated.⁴ Using this procedure, the polar tilt angle of the hemicyanine group for the SP:SA = 1:1 film has been determined. When the surface area was close to the collapse, the obtained polar angle is $\sim 50^{\circ}$ (data not shown). This value is approximately coincident with the θ angle obtained for the hemicyanine group in the SP:DMPA system. The agreement

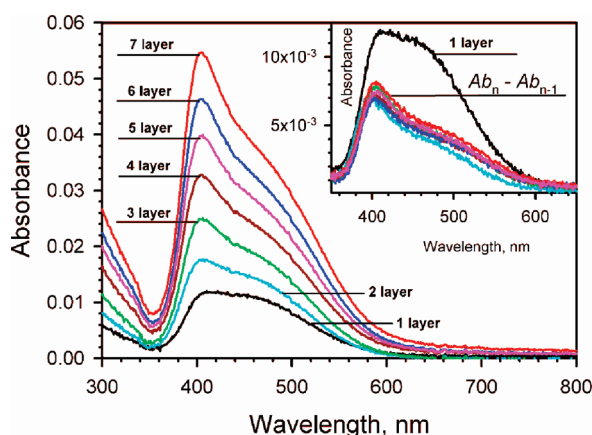


Figure 5. Absorption spectra of 1, 2, ..., 7 SP:SA = 1:1 LS multilayers ($\pi_{\text{Trans}} = 30$ mN/m). The number of the transferred layers is indicated in the figure. Inset: Spectrum of the first monolayer and the subtracted spectra of the following layers ($Ab_n - Ab_{n-1}$). Similar line colors are used to indicate the number of layers used in both graphs.

between these values can be pointed out qualitatively by collating the spectra obtained for the SP:SA and SP:DMPA films at 0.41 and 0.63 nm², respectively (see Figure 4). A simple visual comparison of these spectra allows one to observe that the integration of the visible band should provide similar areas for both systems and, therefore, similar polar angles. However, similar values of the tilt polar angle of the hemicyanine group in both cases is contradictory, since the areas occupied by this group are quite different in the SP:SA and SP:DMPA films. In fact, the tilt angle of this group can be determined by geometric models, obtaining $\sim 35^\circ$ when the projected area of the hemicyanine group over the interface was ~ 0.4 nm². This estimation drastically contradicts the angle calculated from the integration of the band.

The method used to determine the tilt angle of the chromophore, which is based on the integration of the band, provides only an average angle.^{4,22} This average angle can be directly related to the chromophore tilt angle, provided that two conditions are fulfilled: First, there must be only one type of aggregate, with all molecules equally oriented, which can be often achieved at the air–water interface. Second, the band should be simple, i.e., caused by a single transition or at least all transitions of the band with their transition dipoles oriented in the same direction. In the case of failure to comply with these requirements, the angle obtained by the above method would be only an average value of complex interpretation.

4. Transmission Spectra of the Mixed SP:SA LS Films. Langmuir monolayers of SP:SA = 1:1 have been transferred onto quartz supports at different constant surface pressures, π_{Trans} , using the LS method. Transmission spectra of the LS films have been obtained under normal and 45° incidence angle, with nonpolarized, s-, and p-polarized light. Figure 5 shows the spectra for the first 7 monolayers transferred at $\pi_{\text{Trans}} = 30$ mN/m, recorded under normal incidence.

The maximum value for the absorption spectra increased monotonically with increasing the number of transferred monolayers. The inset in Figure 5 shows the spectrum of the first monolayer (black line), as well as the spectra obtained by subtracting two successive spectra ($Ab_n - Ab_{n-1}$). The subtracted spectra ($Ab_n - Ab_{n-1}$) were almost coincident for any n

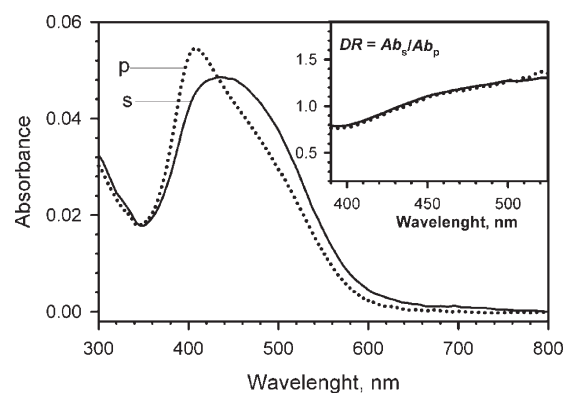


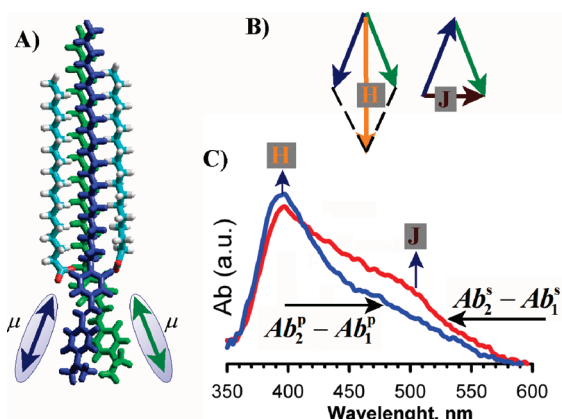
Figure 6. s- and p-polarized transmission spectra of 7 LS monolayers of SP:SA = 1:1, obtained under an incidence of 45° and transferred at $\pi_{\text{Trans}} = 30$ mN/m. Inset: The variation of DR at the 390–520 nm region (solid line). The DR after subtraction of the s and p spectra of the first monolayer is also shown with a dotted line.

transferred monolayer, although a quite different spectrum was obtained for the first monolayer. The transference of monolayers has been performed at different values of π_{Trans} . The results indicated that both the shape and height of the first monolayer spectrum depended on the transfer pressure. However, for $\pi_{\text{Trans}} \geq 7$ mN/m, the shape and height of the subtracted spectra were independent of the transfer pressure. Also, the shapes of the subtracted spectra were consistent with those of the reflection spectra recorded close to collapse. Consequently, the interactions between the monolayer and the support account for the changes observed in the spectra of the first monolayer transferred at different π_{Trans} . However, once the quartz surface was coated with the first monolayer, the subsequent films transferred did not change the structure that they had at the air–water interface. The molecular organization refers here to the arrangement of the hemicyanine group.

To rule out anisotropy in the plane of the quartz substrate, at least on the area covered by the footprint of the incident light beam, spectra were recorded under normal incidence of light at different polarization angles. The obtained spectra were identical in all cases. Figure 6 shows the transmission spectra of 7 monolayers obtained under an incidence of 45° and s- and p-polarized light. The shape of the spectra under s- and p-polarized light changed appreciably. Thus, while the s spectrum was a broadband centered at ~ 435 nm, the p spectrum had a narrow band centered at 405 nm and a shoulder at ~ 510 nm. The dichroic ratio, $DR = Ab_s / Ab_p$, is shown as an inset in Figure 6 (solid line). The DR after the subtraction of the s and p spectra of the first monolayer is also shown (dotted line). The DR ratio varied from the values of 0.8 for $\lambda \approx 405$ nm to 1.35 for $\lambda \approx 510$ nm. These transfers were repeated at different surface pressures $\pi_{\text{Trans}} \geq 7$ mN/m, and the dichroic ratio ranged in all cases from 0.82 ± 0.04 for $\lambda \approx 405$ nm to 1.35 ± 0.05 for $\lambda \approx 510$ nm. Then, the polarization properties of the band must be related to the coexistence of two transition dipoles with different orientations. The first transition dipole is named the H component, and has the maximum absorption at ~ 405 nm. The second transition dipole is named the J component, and has the maximum absorption at ~ 510 nm, (see Scheme 2C below, where the s and p subtracted spectra $Ab_2 - Ab_1$ are shown).

For very thin films, i.e., for weak absorption values ($<1\%$), and according to Vandevyver et al.,²⁷ the dichroic ratio DR can be

Scheme 2. (A) Hemicyanine Aggregation Model Sketch, Where μ Represents the Transition Dipole, (B) the Two Optically Allowed Components of the Addition of the Transition Dipole, and (C) Spectra Obtained by Subtracting the s- and p-Polarized Light Spectra Obtained from the Second and First Monolayer ($Ab_2 - Ab_1$)



expressed as:

$$DR = \frac{Ab_s}{Ab_p} = \frac{\left[\frac{n_1 \cos(r) + n_3 \cos(i)}{n_1 \cos(i) + n_3 \cos(r)} \right] \left[\frac{n_2^4 \langle \sin(\theta)^2 \rangle}{2n_1^3 n_3 \sin(i)^2 \langle \cos(\theta)^2 \rangle + n_2^4 \langle \sin(\theta)^2 \rangle \cos(i) \cos(r)} \right]}{(2)}$$

where n_1 (=1), n_2 and n_3 (=1.43) are the refractive index of air, film, and quartz, respectively, i is the incidence angle of the light, $r = \arcsin[n_1 \sin(i)/n_3]$ is obtained from Snell's ratio, θ is the angle between the transition dipole and the normal to the support, and brackets denote average values. According to eq 2, and using $n_2 = 1.6$,⁴ and $i = 45^\circ$, DR = 1.56 was obtained for $\theta = 90^\circ$ (parallel orientation with respect to the support), while DR = 0 for $\theta = 0^\circ$ (perpendicular orientation).

From eq 2 ($n_2 = 1.6$ and $i = 45^\circ$), the tilt angle from the DR values has been calculated, obtaining $\theta = 32^\circ \pm 2^\circ$ for DR ≈ 0.82 ($\lambda \approx 405$ nm), and $\theta \approx 56^\circ \pm 4^\circ$ for DR ≈ 1.35 ($\lambda \approx 510$ nm). In any case, these values must be carefully considered, since the H and J components of the absorption band could not be completely resolved. The DR variation (Figure 6) confirmed that the method previously used to determine the tilt of the chromophore at the air–water interface, which consisted of the integral of the reflection band, cannot be used for the SP:SA system.

In the present case, there are two possible explanations for the variation of DR in the region of 400–510 nm. The first reason could be the coexistence of various types of aggregates with different orientations with respect to the interface. However, this explanation seemed unlikely. Indeed, in the case of the coexistence of two or more kinds of aggregates, the relative proportion between them should vary with the applied surface pressure, which would be detected by changes in the shape of the spectrum under normal incidence with nonpolarized light. Excluding the effect of the first monolayer transferred, this was not detected in the spectra of the following monolayers. To detect the possible presence of various kinds of aggregates, the emission spectra of the transferred films have been recorded, exciting at 405 and

510 nm. In the case of the coexistence of different types of aggregates, each of them should have different emission properties, and different emission spectra should be obtained. However, the emission of the SP:SA films was not detected under excitation at 405 and 510 nm, which points to the existence of a single type of aggregate. Given the case of coexistence of J and H aggregates, emission from (at least) the J aggregates is expected (Kobayashi, J aggregates books).⁵ Therefore, the absence of emission indicates the occurrence of only H aggregates. Moreover, data obtained by GIXD and IRRAS at the air–water interface support the idea of the existence of a single type of aggregate. As previously commented, GIXD peaks are well-defined, arising from a single crystalline phase. Moreover, the occurrence of different aggregate types would lead to a broadening of the IRRAS bands, as they would arise from different contributions, which is not the case herein.

The second phenomenon that may explain the variation of DR shown in Figure 6 is the existence of inequivalent molecules in the aggregate. This phenomenon has been described previously for molecular crystals according to Davydov's exciton theory, which shows that a given molecular energy level may be split into as many components as there are inequivalent molecules per unit cell.^{7,28} In addition to the spectral splitting, the Davydov bands exhibit distinct polarization properties, as in our case.

Focusing our attention exclusively on two adjacent SP molecules, and in spite of SP molecules counteracting their positive charges with the stearic acid molecules, it can be assumed that the close proximity between hemicyanine groups will lead to a strong repulsion between their dipole moments. To reduce this repulsion energy, the partial rotation of the groups in opposite directions may occur, as shown in Scheme 2A (the two SP molecules are drawn in different colors). In this configuration, the transition dipoles, μ , are not parallel, and the addition of these dipoles gives rise to two optically allowed components: one almost perpendicular to the support (H component) and another almost parallel to the support (component J) (see Scheme 2B). The structure drawn in Scheme 2A is solely a sketch obtained by means of the MM+ method.²⁹ The geometry of SP (positively charged) and SA (stearic acid anion) molecules has been previously optimized by means of the RM1 semiempirical method.³⁰ The results could not be extrapolated to the experimental conditions existing at the air–water interface, but it should be highlighted that the hemicyanine groups are aggregated and slightly twisted by one another in the structure optimized by the MM+ method (see Scheme 2A).

The tilt angles, as determined for the H and J components on the quartz support, cannot be extrapolated directly to the monolayer at the air–water interface: reorientation of the film may happen during the transfer process. However, the shape of the reflection band recorded at the air–water under high surface pressure, and the shape of the absorption band on quartz, once the spectrum of the first monolayer was subtracted, were almost coincident. This fact clearly indicated that the air–water absorption band should have the same polarization properties as the quartz band, i.e. the band is split into its two components H and J. Moreover, on quartz, the angle of the H component, $\theta \approx 32^\circ$, represented the average tilt angle of the hemicyanine transition dipole with respect to the normal of the support. This average angle value was almost coincident with that obtained from geometric considerations at the air–water interface, $\theta \approx 35^\circ$, assuming a projected area of the hemicyanine group over the interface of about 0.4 nm^2 .

For the SP:DMPA monolayer at the air–water interface, the hemicyanine tilt angle has been determined by using the method based on the integration of the reflection band.⁴ To check if the method is successful for this system, monolayers of SP:DMPA = 1:1 have been transferred on quartz substrates by the same procedure as for the SP:SA system. The results indicated that the splitting of the band also exists in the SP:DMPA system, although the J component showed much less intensity in this case. The difference in intensities could be related to a larger separation between hemicyanine groups and, therefore, a lower rotation between them. In addition, the H component absorbed at 460 nm, being the tilt angle on quartz is about 50°, is approximately coincident with the angle previously obtained at the air–water interface.⁴ It can be concluded that the method of integration of the band led to a correct angle value because of the small intensity of the J component.

CONCLUSIONS

The formation of mesoscopic 2D structures from mixed SP:SA = 1:1 monolayers at the air–water interface has been reported and compared with the previously reported structures of the SP:DMPA = 1:1 system.⁴ With regard to the SP:DMPA = 1:1 films, the replacement of DMPA by SA implies reducing the available area for the hemicyanine aggregation, since each SA molecule provides only one alkyl chain to the set, being the minimum perpendicular section of the 1:1 mixture around 0.4 nm² per SP molecule. In the case of the SP:DMPA mixed monolayer, DMPA provided two alkyl chain to the set, with a minimum perpendicular section of the 1:1 mixture around 0.6 nm² per SP molecule.

The SP:SA = 1:1 monolayer forms star-shaped domains, bearing inner textures, related to anisotropy. The anisotropy is provoked by the absorption of the polar group. The anisotropy is related to a high degree of order in the interface. Therefore, the SP:SA mixed monolayer might be defined as a 2D molecular crystal. However, for the SP:DMPA = 1:1 film circular domains have been observed. Furthermore, branches grow from circular domains when there is an increase in temperature.

GIXD experiments for the SP:SA = 1:1 system showed that the hydrocarbon chains adopted, at low values of surface pressure, a L_{2h} phase with a small tilt of the hydrocarbon chains in the NN direction. At ~5 mN/m, the chains adopted an untitled conformation with NNN unit-cell distortion. This distortion might be ascribed to the effect of the bulky SP headgroup. The tight packing of the hydrocarbon chains has been further confirmed by IRRAS. Significant changes in the organization of the polar groups when DMPA was replaced by SA in the mixed film were observed by UV–vis spectroscopy. The maximum wavelength of the reflection band shifted from 475 to 410 nm for the SP:SA = 1:1 system, while for the SP:DMPA = 1:1 system the shift was from 475 to 459 nm. The longer shift for SP:SA film was indicative of the greater interaction between the hemicyanine groups in the presence of SA. The splitting of the absorption band has been related to the existence of nonequivalent molecules per unit cell in the aggregate.^{7,28} Thus, the close proximity between hemicyanine groups might cause a strong repulsion between their dipole moments, leading to a partial rotation of the groups in opposite directions. The transition dipoles, μ , are not parallel, resulting in two optically allowed components: one almost perpendicular to the substrate (H component) and another almost parallel to the substrate

(J component). The splitting of the absorption band was not previously observed for the SP:DMPA film because of the lower intensity of the component J, caused by both the greater separation between hemicyanine groups and the least amount of tilt between them.

The changes observed by replacing DMPA for SA in the mixed monolayer should relate primarily to the less area available for the folding and hemicyanine aggregation. A high packing of alkyl chains for both mixed monolayers has been observed by GIXD. The anisotropy of the domains is caused by the polar groups. The anisotropy is related to a high degree of order and packing of such groups (molecular crystal). The splitting of the absorption band supports this idea.

The domain shape mainly originates from the interactions between the polar groups and the limitations of available space in this region of the monolayer. The interactions between the alkyl chains are fundamental in maintaining the crystal structure formed, but they do not appear to play the main role in the final geometry of the domain.

ASSOCIATED CONTENT

S Supporting Information. IRRAS spectra from the mixed SP:SA monolayer in a 1:1 molar ratio at $T = 21^\circ\text{C}$, at different surface pressures. This material is available free of charge via the Internet at <http://pubs.acs.org>.

AUTHOR INFORMATION

Corresponding Author

*E-mail: lcamacho@uco.es.

ACKNOWLEDGMENT

The authors thank the Spanish CICYT for financial support of this research in the framework of Projects CTQ2007-64474 and CTQ2010-17481 and also thank the Junta de Andalucía (Consejería de Innovación, Ciencia y Empresa) for special financial support (P08-FQM-4011). A. González-Delgado thanks the Ministerio de Ciencia e Innovación for a predoctoral grants (FPI program) and Juan J. Giner-Casares acknowledges the Alexander von Humboldt Foundation for a postdoctoral fellowship.

REFERENCES

- (1) Johann, R.; Vollhardt, D.; Möhwald, H. *Colloid Polym. Sci.* **2000**, 278, 104.
- (2) Vollhardt, D.; Liu, F.; Rudert, R. *J. Phys. Chem. B* **2005**, 109, 17635.
- (3) Giner-Casares, J. J.; de Miguel, G.; Pérez-Morales, M.; Martín-Romero, M. T.; Muñoz, E.; Camacho, L. *J. Phys. Chem. C* **2009**, 113, 5711.
- (4) González-Delgado, A. M.; Rubia-Paya, C.; Roldán-Carmona, C.; Giner-Casares, J. J.; Perez-Morales, M.; Muñoz, E.; Martín-Romero, M. T.; Camacho, L.; Brezesinski, G. *J. Phys. Chem. C* **2010**, 114, 16685.
- (5) Kobayashi, T. *J-Aggregates*; World Scientific: Singapore, 1996.
- (6) Kuhn, H.; Försterling, H. D. *Principles of Physical Chemistry*; John Wiley & Sons: New York, 1999.
- (7) Pope, M.; Swenberg, C. E. *Electronic Processes in Organic Crystals and Polymers*; Oxford Science Publications: New York, 1999.
- (8) Grüniger, H.; Möbius, D.; Meyer, H. *J. Chem. Phys.* **1983**, 79, 3701.
- (9) Kaganer, V. M.; Peterson, I. R.; Kenn, R. M.; Shih, M. C.; Durbin, M.; Dutta, P. *J. Chem. Phys.* **1995**, 102, 9412.

- (10) Jaquemain, D.; Leveiller, F.; Weisbuch, S.; Lahav, M.; Leiserowitz, L.; Kjaer, K.; Als-Nielsen, J. *J. Am. Chem. Soc.* **1991**, *113*, 7684.
- (11) Als-Nielsen, J.; Jaquemain, D.; Kjaer, K.; Lahav, M.; Levellier, F.; Leiserowitz, L. *Phys. Rep.* **1994**, *251*.
- (12) Kjaer, K. *Phys. B* **1994**, *198*, 100.
- (13) Brezesinski, G.; Dietrich, A.; Struth, B.; Böhm, C.; Bouwman, W. G.; Kjaer, K.; Möhwald, H. *Chem. Phys. Lipids* **1995**, *76*, 145.
- (14) Kaganer, V. M.; Möhwald, H.; Dutta, P. *Rev. Mod. Phys.* **1999**, *71*, 779.
- (15) Muentner, A. H.; Hentschel, J.; Börner, H. G.; Brezesinski, G. *Langmuir* **2008**, *24*, 3306.
- (16) Flach, C. R.; Gericke, A.; Mendelsohn, R. *J. Phys. Chem. B* **1997**, *101*, 58.
- (17) Bibo, A. M.; Knobler, C. M.; Peterson, I. R. *J. Phys. Chem.* **1991**, *95*, 5591.
- (18) Brezesinski, G.; Vollhardt, D.; Iimura, K.; Cölfen, H. *J. Phys. Chem. C* **2008**, *112*, 15777.
- (19) Socrates, G. *Infrared and Raman Characteristic Group Frequencies: Tables and Charts*; John Wiley & Sons: Weinheim, Germany, 2001.
- (20) Orrit, M.; Möbius, D.; Lehmann, U.; Meyer, H. *J. Chem. Phys.* **1986**, *85*, 4966.
- (21) Martín, M. T.; Prieto, I.; Camacho, L.; Möbius, D. *Langmuir* **1996**, *12*, 6554.
- (22) Pedrosa, J. M.; Martín-Romero, M. T.; Camacho, L.; Möbius, D. *J. Phys. Chem. B* **2002**, *106*, 2583.
- (23) Song, Q.; Evans, C. E.; Bohn, P. W. *J. Phys. Chem.* **1993**, *97*, 13736.
- (24) Lusk, A. L.; Bohn, P. W. *Langmuir* **2000**, *16*, 9131.
- (25) Lusk, A. L.; Bohn, P. W. *J. Phys. Chem. B* **2001**, *105*, 462.
- (26) Hall, R. A.; Thistlethwaite, P. J.; Grieser, F.; Kimizuka, N.; Kunitake, T. *Colloids Surf., A* **1995**, *103*, 167.
- (27) Vandevyver, M.; Barraud, A.; Ruaudel-Teixier, A.; Maillard, P.; Gianotti, C. *J. Colloid Interface Sci.* **1982**, *85*, 571.
- (28) Davydov, A. S. *Theory of Molecular Excitons*; McGraw-Hill: New York, 1962.
- (29) *Hyperchem*, 6th ed.; Htpercube, Inc.: Gainesville, FL, 1999.
- (30) Rocha, G. B.; Freire, R. O.; Simas, A. M.; Stewart, J. J. P. *J. Comput. Chem.* **2006**, *27*, 1101.